Spine

SPINE Volume 43, Number 19, pp E1116–E1126

BIOMECHANICS

The Influence of Concordant Complex Posture and Loading Rate on Motion Segment Failure

A Mechanical and Microstructural Investigation

Meredith L. Schollum, PhD,* Kelly R. Wade, PhD,* Zhi Shan, MD,† Peter A. Robertson, MD,‡ Ashvin Thambyah, PhD,* and Neil D. Broom, PhD*

Study Design. Microstructural investigation of compression-induced herniation of a lumbar disc held in a concordant complex posture.

Objective. To explore the significance of loading rate in a highly asymmetric concordant posture, comparing the mechanisms of failure to an earlier study using a nonconcordant complex posture.

Summary of Background Data. A recent study with a nonconcordant complex posture (turning in the opposite direction to that which the load is applied) demonstrated the vulnerability of the disc to loading that is borne by one set of oblique-counter oblique fiber sets in the alternating lamellae of the annulus, and aggravated by an elevated loading rate. Given the strain rate–dependent properties of the disc it might be expected that the outcome differs if the posture is reversed.

Methods. Forty-one motion segments from ovine 16 spines were split into two cohorts; adopting the previously employed low rate (40 mm/min) and surprise rate (400 mm/min) of loading. Both groups of damaged discs were then analyzed microstructurally.

Results. With the lower rate loading the concordant posture significantly *reduced* the load required to cause disc failure than earlier described for nonconcordant posture (6.9 *vs.* 8.4 kN), with more direct tears and alternate lamella damage extending to the anterior disc. Contrary to this result, with a surprise rate, the load at failure was significantly *increased* with the concordant posture (8.08 *vs.* 6.96 kN), although remaining significantly less than that from a simple flexed posture (9.6 kN). Analysis of the damage modes and postures suggest facet engagement plays a significant role.

Conclusion. This study confirms that adding shear to the posture lowers the load at failure, and causes alternate lamella rupture. Load at failure in a complex posture is not determined by loading rate alone. Rather, the strain rate–dependent properties of the disc influence which elements of the system are brought into play.

Key words: annular disruption, asymmetric posture microstructural analysis, complex posture, compression, mechanism of herniation, ovine lumbar motion segments.

Level of Evidence: N/A

Spine 2018;43:E1116–E1126

As we try to understand the biomechanics of the disc with the hope of replacing it with either a prosthetic joint or a tissue engineered material, the microstructure and the significance of the natural design of the disc should not be understated. It is also vitally important to understand its limitations to minimize the risk of damaging this crucial load-bearing organ. Epidemiological studies have emphasized the role three-dimensional trunk motions in low back disorders in industrial settings,[1,2] and recent *in vitro* studies[3,4] have shown a lower load at failure as well as alternate lamellae rupture in ovine motion segments overloaded in a complex posture. These studies employed a nonconcordant posture involving turning in the opposite direction to that which the load is applied (when one turns to the left and pulls from the right) and two loading rates. Unlike simple flexion, the average load at failure in the nonconcordant complex posture was lowered at the elevated rate.

It is well established that heavily hydrated connective tissues such as the intervertebral disc and articular cartilage display strong strain rate–dependent mechanical properties.[5–7] The complex posture introduces significant *shear*, which has the potential to bring the protective function of the facets into play. Therefore, the suggestion that high-rate

From the *Department of Chemical and Materials Engineering, Experimental Tissue Mechanics Laboratory, University of Auckland, Auckland, New Zealand; †Department of Orthopaedic Surgery, Sir Run Run Shaw Hospital, Zhejang University, Hangzhou, China; and ‡Department of Orthopaedic Surgery, Auckland City Hospital, Auckland, New Zealand.

Acknowledgment date: November 3, 2017. First revision date: January 25, 2018. Second revision date: March 6, 2018. Acceptance date: March 13, 2018.

The manuscript submitted does not contain information about medical device(s)/drug(s).

NuVasive funds were received in support of this work.

Relevant financial activities outside the submitted work: consultancy, grants.

Address correspondence and reprint requests to Meredith L. Schollum, PhD, Department of Chemical and Materials Engineering, University of Auckland, Private Bag 92019, Auckland 1142, New Zealand;
E-mail: Meredith.schollum@auckland.ac.nz

DOI: 10.1097/BRS.0000000000002652

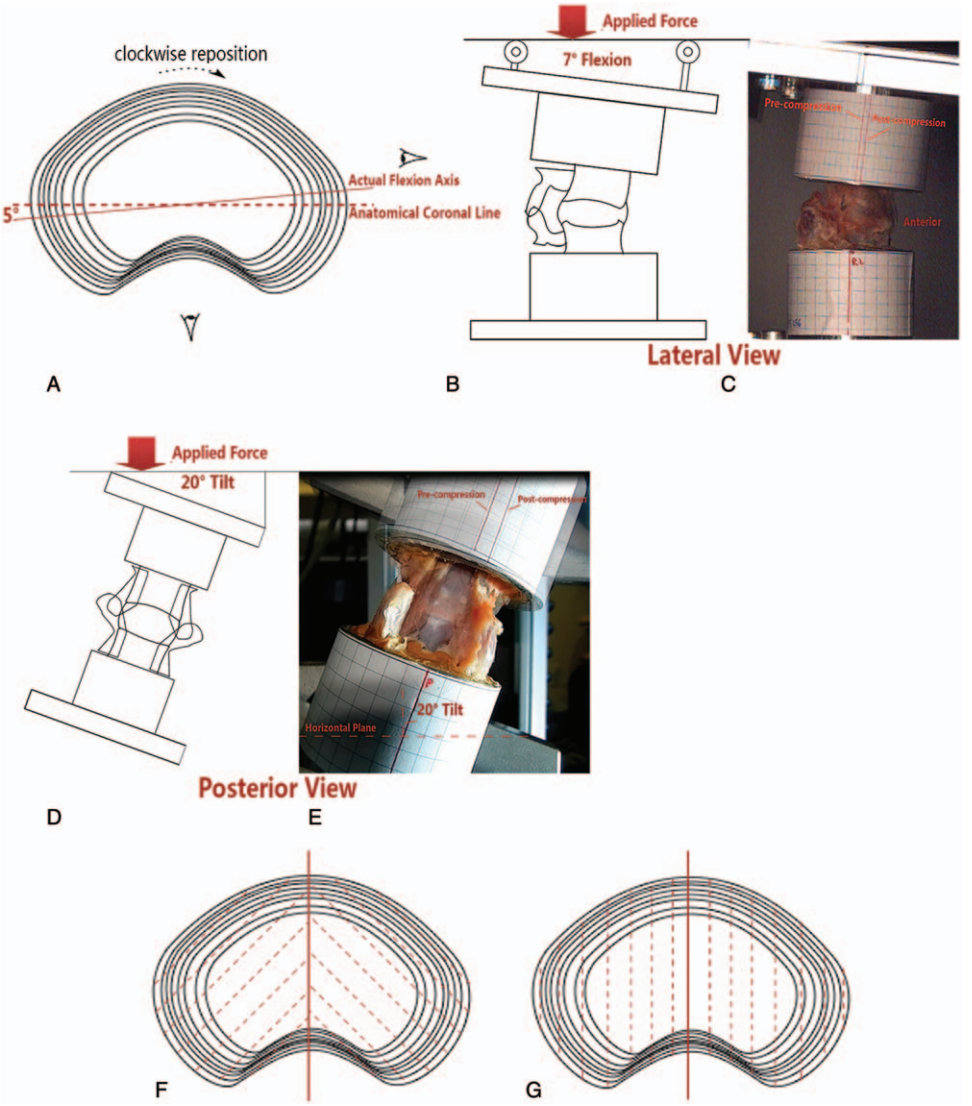

Figure 1. The comp0lex posture incorporated a 5° clockwise rotation of the motion segment in the rig (**A**), 7° of forward flexion (**B, C**), and a 20° right lateral tilt (**D, E**). Note the offset flexion axis adds an element of left lateral bend. **C, E,** Overlaid images of pre- and postcompression of the same segment from lateral and posterior views, respectively. **F**, **G,** The two section planes employed: 45° sagittal and sagittal [Adapted from Ref.[4]].

loading allows less time for fluid pressure equalization and load-sharing across the disc[8] should lead to facet engagement becoming a key factor in load bearing. To test this hypothesis necessitates altering the engagement of the facets before overloading the motion segment in a posture with significant shear. This new investigation achieves this by adopting the same two loading rates as the earlier complex loading studies[3,4] but with a concordant posture (*i.e.*, turning in the *same* direction to that which the load is applied).

MATERIALS AND METHODS

Ovine lumbar spines (2–4 years old) were stored for up to 6 months at −28°C before separating into L1–2, L3–4, and L5–6 motion segments. Using frozen specimens is standard practice in this field[9–11] it does not alter the overall mechanical properties much even over multiple freeze-thaw cycles.[12] The facets were preserved but spinous and transverse processes removed. Macroscopic inspection of the transected discs revealed no evidence of lumbar spine degeneration. Bisecting adjacent discs provides a guide of overall spine health, and any substantial degeneration, that is, dry or disrupted nucleus, irregular annulus. With an age range of 2 to 4 years we have found that any obvious degeneration is a rare occurrence. Following rehydration for 20 hours in physiological saline at 4°C each motion segment was potted in stainless steel cups with dental plaster and maintained hydrated until tested.

Our objective was to approximate the situation of a subject presenting clinically with disc damage following both leaning and rotating to the right and bending forward to lift a heavy load. A rig used in previous investigations[10,13] was adapted to subject discs to an offset compression force whilst rotated to drive the disc to its limits of motion governed by the facet joints, and then compress to failure in this posture (Figure 1).

Each potted segment was positioned in the rig with its long axis tilted laterally 20° (to the right, Figure 1D, E) as a means of applying a component of lateral shear when compressed. The whole segment was then rotated 5° clockwise as viewed from above (Figure 1A). Finally, 7° of flexion, approximately

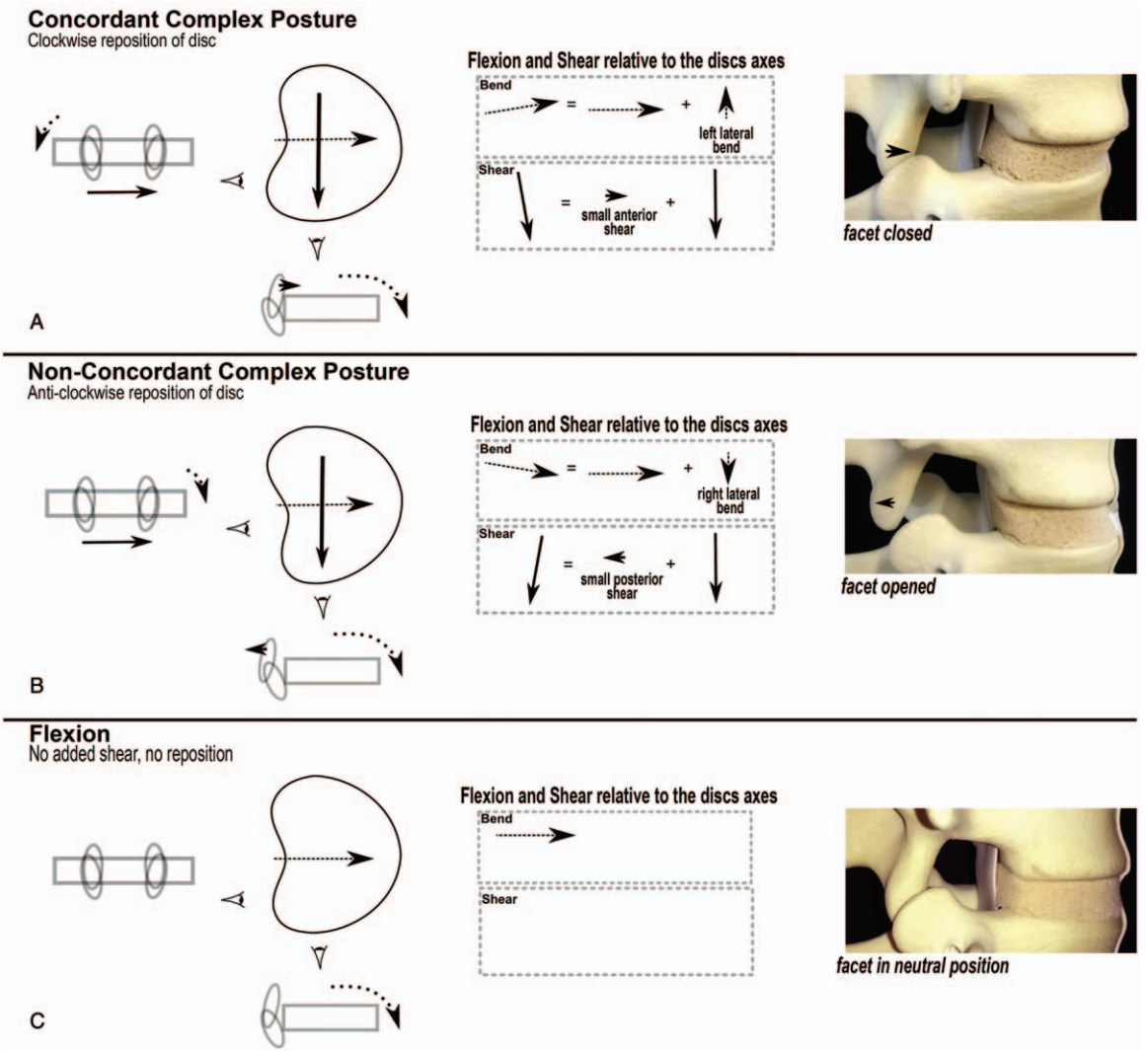

Figure 2. Plan, posterior, and lateral views of the imposed flexion and shear for three postures. **A**, concordant complex, note the major right lateral shear has an element of anterior shear, closing the facets. **B**, Nonconcordant complex, here the major right lateral shear has an element of posterior shear, opening the facets. **C**, Flexed. Dashed arrows = imposed flexion, solid arrows = imposed shear. The boxed vectors represent the flexion and shear relative to the discs sagittal and coronal axes.

the limit of physiologic flexion for ovine discs,[14] was applied in the plane corresponding to the original sagittal plane of the motion segment before it was rotated (Figure 1B, C). The flexion in this plane, being offset to the disc's sagittal plane, had the effect of adding a small component of lateral bend. Schematics indicating the directions of the imposed shear and flexion for both this new study and the previous flexed and nonconcordant studies are shown in Figure 2A–C.

Testing was done at two loading rates; 40 mm/min, and a "surprise" rate of 400 mm/min which approximates the maximum rate of muscle activation.[15,16] Samples were compressed using a materials testing machine (Instron 5567) under load control and test termination criteria were adopted from previous studies[10,13] these being either 15% load drop or a driven displacement of 3 mm, whichever came first. Shear and bending measurements were obtained using two video cameras positioned with respect to the primary axes of rotation.

For the 40 mm/min cohort, 20 motion segments from 8 spines were tested. Based on the load-displacement curves, all tests were terminated either at the peak load or following a drop in load. For the 400 mm/min cohort, 21 motion segments from 8 spines were tested. Three tests were terminated before any drop in load (early stage) thus providing insight into the early stages of failure. Of the possible 24 segments in each cohort, a total of six tests failed to comply with the testing protocol; four due to plastering errors, one with an incorrect alignment in the testing rig, and one was demolished due to a failure to set the end-of-test criteria. A seventh segment was rejected as deformed, with osteophytes present on this level alone.

Following testing, each segment was trimmed to isolate the disc and its adjacent end plates, fixed in 10% formalin and decalcified in 10% formic acid. Each sample was then cryosectioned to obtain 30 μm thick sections along one of two planes (Figure 1F, G); the "45° sagittal plane" (13 of

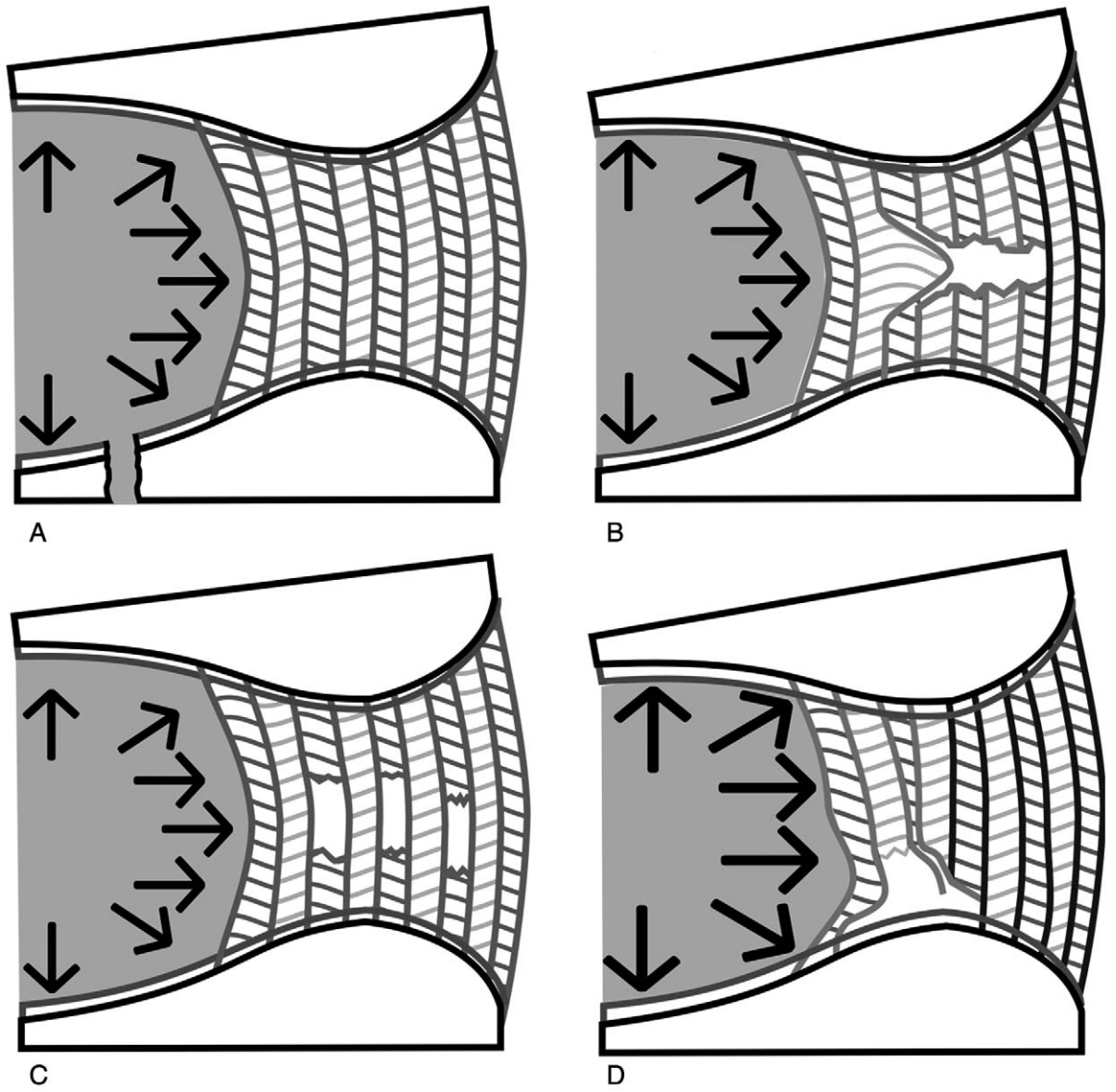

Figure 3. Motion segments contained one or more of these four types of damage. **A**, Endplate fracture (V) in which the osseous endplate itself was broken and the resulting defect penetrates the vertebral body. **B**, Mid-span direct tearing (M_d) in which the annular wall suffered rupture spanning several adjacent lamellae. **C**, Mid-span noncontinuous tearing (M_{nc}) in which several alternate lamellae ruptured. **D**, Annulus-endplate tears (ET) which involved damage to the annulus-endplate junction [Adapted from Ref.[4]].

40 mm/min cohort, 17 of 400 mm/min cohort) which minimized central posterior and lateral annulus trimming losses, and the ''sagittal plane'' (7 of 40 mm/min cohort, 4 of 400 mm/min cohort) allowing direct comparison to earlier studies. Slices were imaged fully hydrated using differential interference contrast optical microscopy. Between 12 and 18 sections were examined per half disc block at 0.7 mm intervals. Note, growth plate status is ascertained during the microstructural analysis.

Failure modes were recorded according to location and type (Figure 3A–D). All failure data were compared with published nonconcordant complex loading studies,[3,4] and simple flexion studies[13] at the same 40 and 400 mm/min rates (Table 1 and Figure 4 A–C). Because of the strict load termination criteria employed facet fractures under such conditions can be easily missed. Careful reanalysis of the 400 mm/min nonconcordant tests[3] terminated after peak load revealed right facet fractures in 7 of 30 segments.

Independent *t* test or analysis of variance was used to compare mean data among groups, with differences between groups analyzed using the least significant difference *post hoc* analysis. Statistical analyses were performed using SPSS 21.0 (IBM Corp., Armonk, NY). $P < 0.05$ was considered significant.

RESULTS

Mechanical Observations

Table 1 lists the failure loads for samples subjected to the concordant complex loading, together with the published

TABLE 1. Comparison of Motion Segment Failure by Compression at Two Loading Rates With: a Concordant Complex Posture, Alongside Previously Published Nonconcordant Complex Posture and Flexed Posture

	Complex, Concordant		Complex, Nonconcordant		Flexion	
	Low Rate	High Rate	Low Rate*	High Rate†	Low Rate‡	High Rate§
Posture	7° Flexion, 20° offset compression, 5° clockwise axis rotation	7° Flexion, 20° offset compression, 5° clockwise axis rotation	7° Flexion, 20° offset compression, 5° anti-clockwise axis rotation	7° Flexion, 20° offset compression, 5° anti-clockwise axis rotation	10° Flexion, vertical compression	10° Flexion, vertical compression
Loading rate (mm/min)	40	400	40	400	40	400
Segments tested (including early stage termination)	20(20)	18(21)	21 (30)	30 (37)	19 (24)	16 (24)
Load at failure (kN)	6.93 SD 0.94 (5.21–8.69)	8.08 SD 1.76 (4.73–11.60)	8.42 SD 1.22 (5.93–10.92)	6.96 SD 1.48 (3.58–9.82)	9.69 SD 2.56 (6.10–15.00)	9.58 SD 1.96 (5.92–12.91)
	Prevalence of damage types¶					
Vertebral fracture, *V*	5 (25%)	12 (67%)	7 (33.3%)	16 (53.3%)	9 (47.4%)	4 (25.0%)
Alternate lamella rupture, M_{nc}	20 (100%)	16 (89%)	21 (100%)	30 (100%)	1 (5.26%)	1 (6.3%)
Direct radial tearing, M_d	19 (95%)	15 (83%)	8 (38.1%)	29 (96.7%)	6 (31.6%)	4 (25.0%)
Disc-endplate tearing, ET	10 (50%)	8 (44%)	9 (42.9%)	10 (33.3%)	3 (15.8%)	9 (56.3%)
Anterior annular tearing	18 (90%)	15 (83%)	2 (6.7%)	24 (80%)	0 (0%)	1 (6.3%)
Facet fracture	0 (0%)	12 (67%)	0 (0%)	7 (23%)	0 (0%)	0 (0%)

*Data from Table 2 [Wade, 2017].

†Data from Table 2 [Shan, 2017].

‡Data from Table 2 [Wade, 2014], "Neutral + high rate," endplate failure and disc herniation combined, with five early stage tests (detailed in Table 3) excluded.

§Data from Table 2 [Wade, 2014].

¶Only those tests terminated after peak load were counted.

nonconcordant complex loading studies,[3,4] and simple flexion studies.[13] The average peak load under 400 mm/min concordant complex loading (8.08 kN) was significantly higher than at 40 mm/min (6.93 kN) as well as 400 mm/min nonconcordant (6.96 kN) but significantly lower than simple flexion at either rate (9.69 and 9.58 kN) and not significantly different to 40 mm/min nonconcordant complex loading (8.42 kN).

Damage types for samples subjected to the concordant complex loading are presented graphically in Figure 4, alongside nonconcordant complex loading studies, and simple flexion studies.

With a 40 mm/min loading rate the average induced shear was 2.1 mm (standard deviation [SD] 0.15 mm) to the right, 1.4 mm (SD 0.17 mm) anteriorly, and 0.8° (SD 0.18°) of left lateral bend. At 400 mm/min, the average induced shear was 4.8 mm (SD 0.23 mm) to the right, 3.05 mm (SD 0.52 mm) anteriorly, and 1.13° (SD 0.15°) of left lateral bend.

The facet joint bony structures of all 40 mm/min loaded segments (n = 20) survived the test intact. But of the 400 mm/min tests terminated after peak load (n = 18), 12 of these presented with right superior facet fractures.

Microstructural Analysis of Damage

Damage types for all 20 40 mm/min tested motion segments and all 21 400 mm/min tested motion segments are summarized in Table 1 and Figure 4A.

Low Rate

General Patterns of Disruption for Tests Terminated After Peak Load

All 20 segments (100%) contained alternate lamella ruptures. Direct radial rupture within the mid-annulus occurred in 19 samples (95%) disproportionally effecting the left side of the disc (90% *vs.* 50%). Vertebral endplate fracture occurred in five samples (25%), with direct radial tears in the mid-span annulus present in all five of these samples. Disc endplate junction tears were present in 10 samples (50%). Posterior annular failure involving either direct radial or alternate lamella tears, or both, was present in 19 samples (95%)

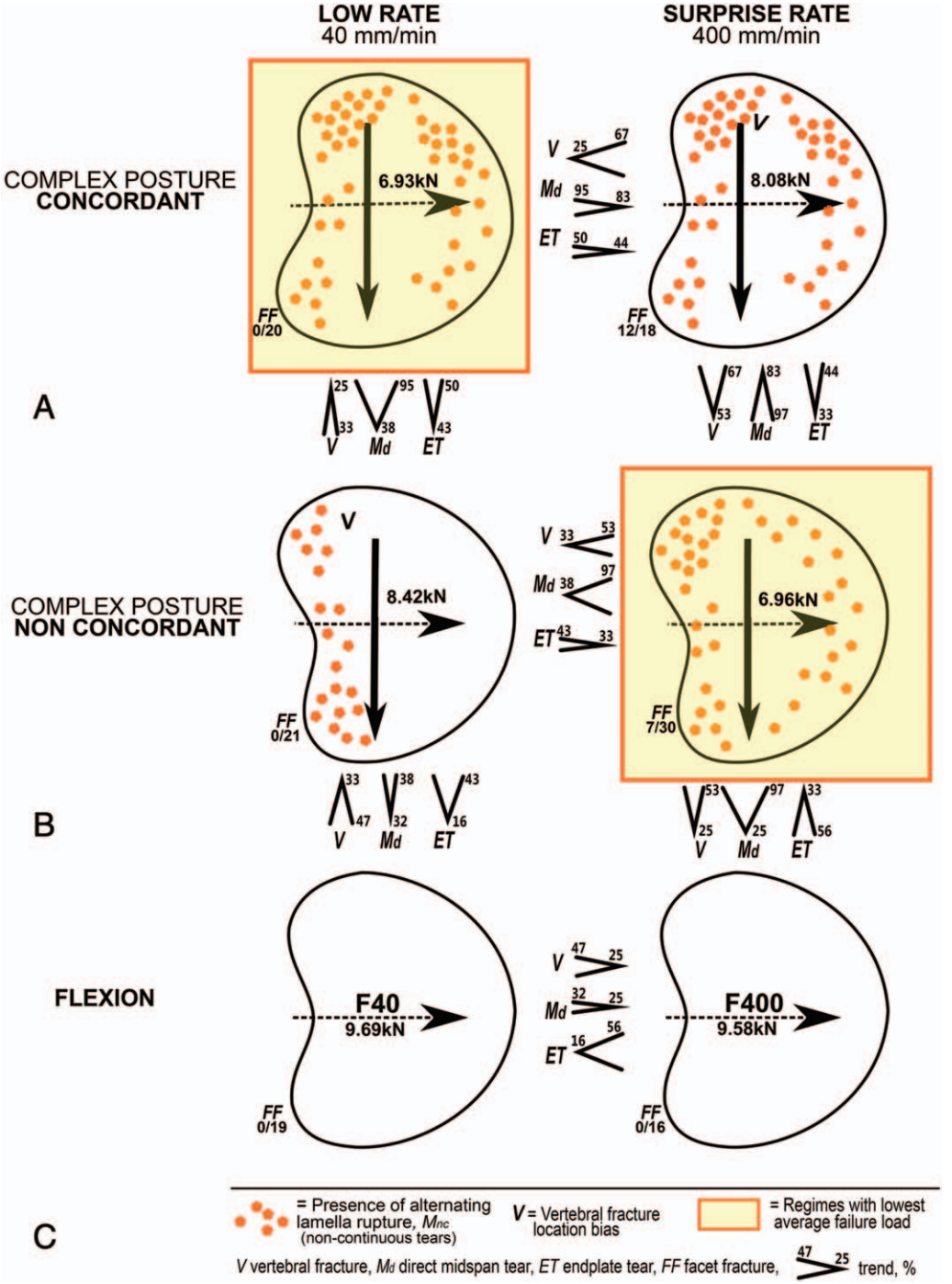

Figure 4. Graphic comparison of motion segment failure by compression at two loading rates with: (**A**) a concordant complex posture, (**B**) a nonconcordant complex posture (previously published[3,4]), and (**C**) a flexed posture (previously published[7]). The occurrence of alternate lamella rupture (M_{nc}) is represented by orange dots, note its absence when compressed in a flexed posture. The occurrence of all other damage types (vertebral fractures, *V*, mid-span direct tears, M_d, and Endplate Tears, ET) are detailed between the schematics as a percentage of tests, with comparison to the neighbouring regime indicated. Facet fracture incidence is also detailed for each regime.

and anteriorly in 18 samples (90%). The anterior annular tears were disproportionally found on the left side; 17 samples (85%) *versus* 11 samples (55%) on the right.

Image Sets Illustrating Damage Types

In addition to a catastrophic posterior direct tear (hollow arrow), Figure 5A and B demonstrates anterior damage at the low rate in the concordant posture (small arrow) affecting alternate lamellae. Further laterally the alternate lamella ruptures are accompanied by ''overextended'' alternate lamellae in the mid to outer annular wall (Figure 5C). Not restricted to the anterior disc wall, short sections of overextended alternate lamellae in a posterior quadrant can be seen Figure 5D and E.

Figure 5. Left side slices from two discs subjected to 40 mm/min concordant complex loading. Centrally the first disc, shown in (**A**), contains a direct radial tear posteriorly (*hollow arrow*), and alternate lamella ruptures anteriorly (*small arrow)*. Further laterally in the same disc (**B**), the tearing is much less severe, persisting anteriorly only as alternate lamella ruptures (*small arrow)*, accompanied by ''overextended'' alternate lamellae in the outer to mid-annular wall. This ''overextension'' (between *asterisks*) is shown at higher magnification in part (**C**), as indicated by the boxed region. A posterolateral example of ''overextension'' effecting a short length of otherwise normal looking lamellae can be seen in (**D**), shown at higher magnification in (**E**) as indicated by the boxed region (between *asterisks*).

Lateral damage was also common in these low rate concordant posture overloaded discs. Figure 6A shows ''overextended'' alternate lamellae captured on a 45° sagittal section plane; Figure 6B illustrates pockets of nuclear material associated with the ruptured alternate lamellae.

Surprise Rate

General Patterns of Disruption for Tests Terminated After Peak Load

Sixteen of 18 segments (89%) contained alternate lamella ruptures. Direct radial rupture within the mid-annulus occurred in 15 samples (83%) again disproportionally effecting the left side of the disc (78% *vs.* 28%). Vertebral endplate fracture occurred in 12 samples (67%), with direct radial tears in the mid-span annulus present in 9 of these samples (75%). Disc-endplate junction tears were present in eight samples (44%). Posterior annular failure involving direct radial, alternate lamella tears, or both, occurred in 16 samples (89%) and anteriorly in 15 samples (83%). The anterior annular tears were more common on the left than the right side; 16 samples (89%) *versus* 12 samples (67%).

Image Sets Illustrating Damage Types

Anterior damage in discs subjected to surprise rate concordant complex loading was evident in very ''early-stage'' failure (*i.e.*, test terminated before any drop in load bearing; Figure 7A). Characteristic of the complex posture loading, alternate ruptured lamellae can be seen anteriorly and posteriorly in Figure 7C and D, respectively. An instance of anterior herniation is captured in Figures 7E and F, with a direct path of nuclear material to the disc periphery.

The near sagittal slice in Figure 8A exemplifies the common situation of multiple types of damage in a disc with a direct tear posteriorly (with evidence of nuclear migration) and outer wall alternate lamella rupture, as well as a superior endplate tear anteriorly alongside alternate lamellae disruption, and ''overextended'' lamellae in the outer wall. Further laterally, extreme ''overextension'' of alternate outerwall lamellae can be seen in near neighbor slices (Figure 8B–D).

DISCUSSION

As with the earlier studies employing complex loading,[3,4] the addition of shear resulted in alternate lamella rupture of the annulus and a lower failure load compared to a simple flexed posture.

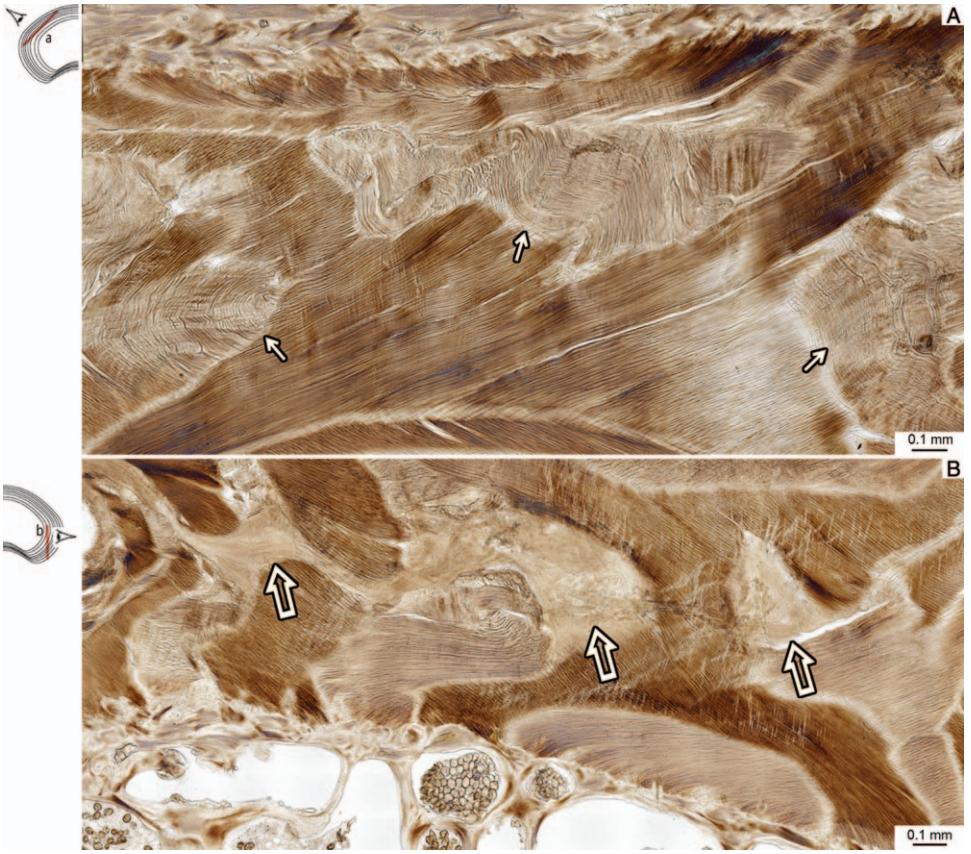

Figure 6. Examples of lateral damage in two discs subjected to 40 mm/min concordant complex loading. In (**A**) is a view of ''overextended'' alternate lamellae (*small arrows*) in the mid to outer left disc wall in a 45° sagittal section plane. The right sagittal slice in (**B**) contains pocketing of nuclear material (*hollow arrows*) in the posterolateral wall.

Inspection of the failure load data for the four groups of complex loaded segments (Table 1, Figure 4) reveals an opposing effect of loading rate, with the average failure load lowest if the loading rate was either ''fast and the posture was nonconcordant'' or ''slow with a concordant posture.'' This contrary effect suggests a difference in load-sharing across the motion segment at different rates. We can explore this proposition by examining the modes of failure with respect to the postures employed.

Consider first the surprise rate data: The average load at failure for the concordant cohort was 8.08 kN and facet fracture was frequent (67%), indicating that the facets were effective in load bearing. Conversely, the nonconcordant high rate cohort had a lower failure load of 6.96 kN, with fewer facet fractures (23%), suggesting that the facets play a lesser protective role. This latter cohort had higher rates of annular tearing with mid-wall direct annular tears present in five of seven of the tests terminated before peak load (early stage), *versus* zero of three for the concordant group.

A further indication that the nonconcordant group has poorly engaged facets, is the substantial increase in direct tearing when the loading rate was increased (38.1% to 96.7%) unlike the concordant posture which had a slight decrease (95% down to 83%). And a contrary pattern was evident with vertebral fractures, which increase modestly from 33.3% to 53.3% as the loading rate was raised, compared to a near three-fold increase in vertebral fractures for the concordant cohort (25% to 67%) alongside elevated facet fractures (nonconcordant 23%, concordant 67%). This increase in both facet and vertebral fractures is likely related, with direct transmission through the bone from overloaded facets potentially causing vertebral fracture.

These results are consistent with the postures described in Figure 2. The nonconcordant posture has right shear plus right lateral bend imposed, serving to open the left facet, allowing greater compression on the left, as seen in the measured left lateral bend (and higher rate of vertebral fractures on the left side at the low loading rate). The element of posterior shear would further serve to disengage the facets. Conversely, for the concordant posture there is an imposed left lateral bend accompanying the right shear, resulting in a more fully engaged left facet, and an element of anterior shear closes the facets.

At low loading rates all facet joints remained intact in the tests, supporting the proposition that the soft tissue elements of the disc are more able to share in the load bearing. However, the direction of offset was again found to be an important factor in the load at failure. The concordant posture adversely engaged the anterior aspect of the disc, reflected in an average failure load of 6.93 kN, with anterior annular tearing present in 90% of segments, compared to 8.42 kN and a 2% rate of anterior annular

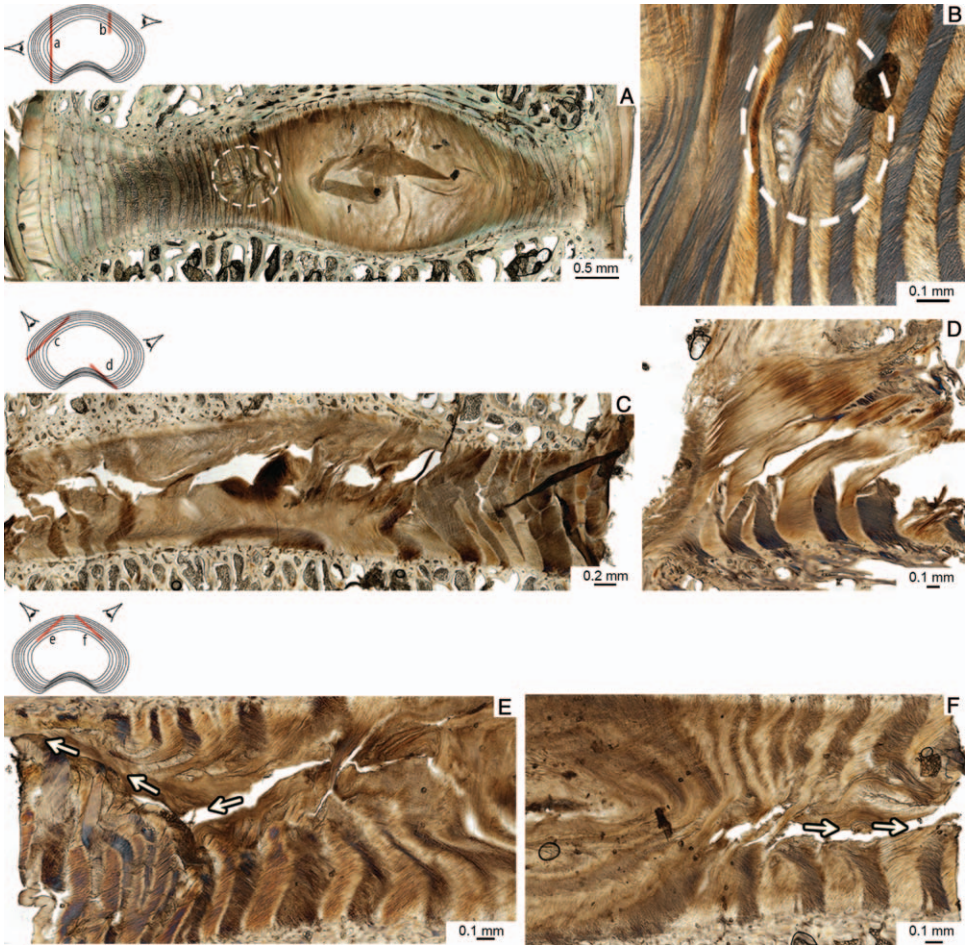

Figure 7. Examples of anterior damage in three discs subjected to 400 mm/min concordant complex loading. The first of these discs was an early-stage failure, with the test halted before any drop in load. The only damage present is inner wall anterior disruption (inside *dashed circle*), both on the left as viewed in (**A**), and on the right as viewed in (**B**). Typical of complex posture loading, the second disc (sectioned on the 45° sagittal plane) presents alternate lamella rupture both left latero-anteriorly (**C**) and right posteriorly (**D**). An example of an anterior herniation is shown in (**E**) and (**F**), with a direct path of nuclear material (*small arrows*) to both the left and right of the centre line.

damage when the posture was nonconcordant at this low rate of loading. Examination of the average shear displacement data shows that very little shear was tolerated for this low rate concordant posture before failure.

If we again consider the posture detailed in Figure 2, the above results can be rationalized. The nonconcordant posture includes an element of posterior shear, likely minimizing load directed to the anterior disc wall. Conversely, the element of anterior shear in the concordant posture may increase the load on the anterior lamellae. The three early-stage high-rate concordant tests, like the nonconcordant study, show non-continuous tears as the first type of damage, but unlike the nonconcordant posture, these tears were evident anteriorly even at the early stage (Figure 7A, B). This supports the proposition that the small anterior shear in the concordant posture is important.

It was proposed in the nonconcordant complex loading study[3] that when there is insufficient time for fluid pressure equalization, the extra length of wall on the left, parallel to the shear direction is critical. This bias to left side damage occurred to a greater extent in this new study, and also at the low loading rate.

The authors were surprised by the amount of ostensibly noncatastrophic lamella extension observed (Figures 5B–E, 6A, 8A–D), affecting approximately 50% of samples to varying degrees. This ''over-extension'' of lamellae was present at both low and high loading rates, appearing most clearly in sagittal sections, and sometimes occurring across quite short sections of a lamella. It was not reported in the earlier nonconcordant studies, suggesting the anterior shear of the concordant posture promotes this damage. A possibility that needs further investigation is that rather than overextended lamellae, they may be recoiled bundles of collagen due to a break out of the plane of the section. The sagittal section planes used do not provide a view of continuous fibers anchoring from vertebra to vertebra. The more dramatic form in the anterior wall as viewed sagittally is likely explained by the near right-angle bisection of the anterior lamellae, offering a clearer view of the anterior wall and any radial deformations.

CONCLUSION

Adding shear to the posture lowers the load at failure, and causes alternate lamella rupture in the annulus. Load at failure in a complex posture is not determined by loading rate alone. Rather, as predicted the strain rate–dependent properties of the disc do influence which elements of the system are brought into play. Under surprise-rate loading the susceptibility to failure is determined by engagement of the facets. Lower loading rates allow time for fluid

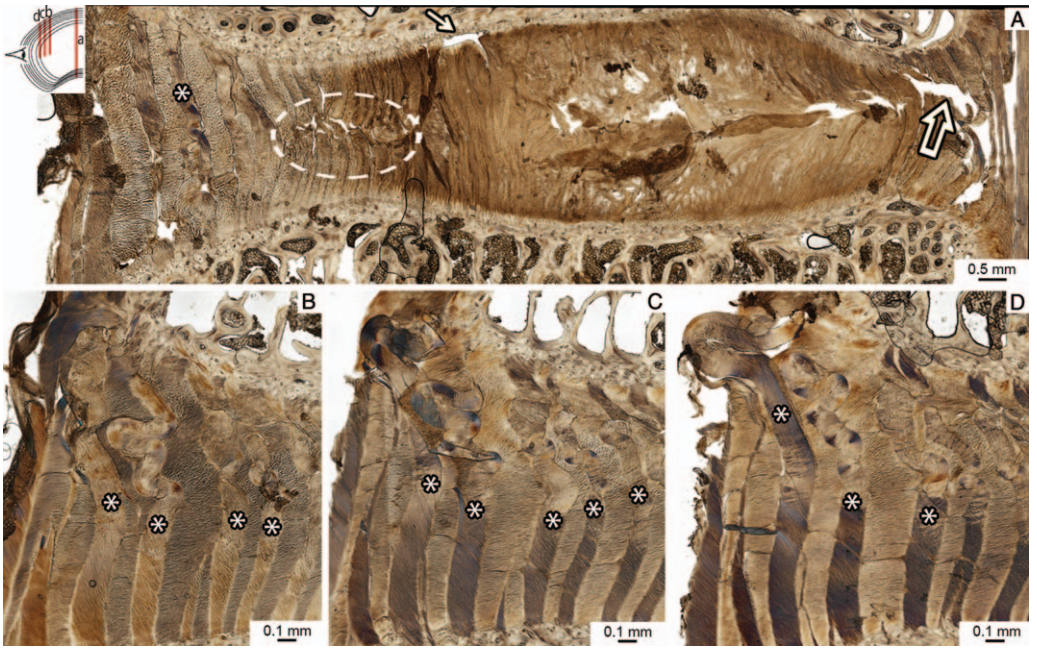

Figure 8. An example of overextended anterior lamellae in a disc subjected to 400 mm/min concordant complex loading. Centrally, in (**A**), there is direct tearing posteriorly (*hollow arrow*), with evidence of nuclear migration to the left, and outer wall noncontinuous tearing to the right. Anteriorly there is both a superior endplate tear (*small arrow*), alternate lamellae disruption in the inner mid wall (*dashed circle*), as well as ''overextended'' lamellae in the outer wall (*asterisk*). Parts (**B**), (**C**), and (**D**) are near neighbor slices of the lateral anterior wall in this disc with extreme amounts of ''overextension'' (effected lamellae marked with *asterisks*).

pressure equalization and here the capacity of the annulus to perform is crucial. Note that the loading rates employed could still be considered modest compared to say a fall from a ladder.

This study has enhanced our understanding of the mechanisms of failure and the vulnerabilities of the motion segment to complex postures and loading rates. It appears that a realistic rate of loading and a common posture (*i.e.*, surprise rate loading with concordant posture) is better tolerated than the more uncommon combinations of rate and posture, implying a highly refined design.

➢ Key Points

- ❑ This study confirms that adding shear to the posture lowers the load at failure, and causes alternate lamella rupture.
- ❑ The poorly engaged facets of the nonconcordant posture appear critical at 400 mm/min, resulting in a low average failure load (6.96 kN) and substantial amounts of direct tearing including anterior tears.
- ❑ At 40 mm/min, switching from a nonconcordant to a concordant posture, resulted in alternate lamella rupture invading the lateral and anterior aspects of the disc, direct tearing becoming widespread (95% *vs.* 35%), and the average load at failure dropping to 6.93 kN (from 8.42 kN).

References

1. Fathallah FA, Marras WS, Parnianpour M. The role of complex, simultaneous trunk motions in the risk of occupation-related low back disorders. *Spine (Phila Pa 1976)* 1998;23:1035–42.
2. Marras WS, Lavender SA, Leurgans SE, et al. The role of dynamic three-dimensional trunk motion in occupationally-related low back disorders: the effects of workplace factors, trunk position, and trunk motion characteristics on risk of injury. *Spine (Phila Pa 1976)* 1993;18:617–28.
3. Shan Z, Wade KR, Schollum ML, et al. A more realistic disc herniation model incorporating compression, flexion and facet-constrained shear: a mechanical and microstructural analysis. Part II: high rate or 'surprise' loading. *Eur Spine J* 2017;26:2629–41.
4. Wade KR, Schollum ML, Robertson PA, et al. A more realistic disc herniation model incorporating compression, flexion and facet-constrained shear: a mechanical and microstructural analysis. Part I: low rate loading. *Eur Spine J* 2017;26:2616–28.
5. Oloyede A, Broom ND. Stress-sharing between the fluid and solid components of articular cartilage under varying rates of compression. *Connect Tissue Res* 1993;30:127–41.
6. Oloyede A, Flachsmann R, Broom ND. The dramatic influence of loading velocity on the compressive response of articular cartilage. *Connect Tissue Res* 1992;27:211–24.
7. Race A, Broom ND, Robertson P. Effect of loading rate and hydration on the mechanical properties of the disc. *Spine (Phila Pa 1976)* 2000;25:662–9.
8. Veres SP, Robertson PA, Broom ND. ISSLS prize winner: how loading rate influences disc failure mechanics: a microstructural assessment of internal disruption. *Spine (Phila Pa 1976)* 2010;35:1897–908.
9. Adams MA, Green TP. Tensile properties of the annulus fibrosus. I. The contribution of fibre-matrix interactions to tensile stiffness and strength. *Eur Spine J* 1993;2:203–8.
10. Wade KR, Robertson PA, Thambyah A, et al. How healthy discs herniate: a biomechanical and microstructural study investigating the combined effects of compression rate and flexion. *Spine (Phila Pa 1976)* 2014;39:1018–28.

11. Veres SP, Robertson PA, Broom ND. The influence of torsion on disc herniation when combined with flexion. *Eur Spine J* 2010;19:1468–78.
12. Pflaster DS, Krag MH, Johnson CC, et al. Effect of test environment on intervertebral disc hydration. *Spine (Phila Pa 1976)* 1997;22:133–9.
13. Wade KR, Robertson PA, Thambyah A, et al. Surprise loading in flexion increases the risk of disc herniation due to annulus-endplate junction failure: A mechanical and microstructural investigation. *Spine (Phila Pa 1976)* 2015;40:891–901.
14. Wilke HJ, Kettler A, Claes LE. Are sheep shines a valid biomechanical model for human spines? *Spine (Phila Pa 1976)* 1997;22: 2365–74.
15. Dolan P, Adams MA. The relationship between EMG activity and extensor moment generation in the erector spinae muscles during bending and lifting activities. *J Biomech* 1993;26:513–22.
16. Mannion AF, Adams MA, Dolan P. Sudden and unexpected loading generates high forces on the lumbar spine. *Spine (Phila Pa 1976)* 2000;25:842–52.